RESEARCH ARTICLE | EARTH, ATMOSPHERIC, AND PLANETARY SCIENCES |

Holocene carbonate record of Lake Kivu reflects the history of hydrothermal activity

Jillian E. Votava, Thomas C. Johnson, and Robert E. Hecky Authors Info & Affiliations

Edited by Thure E. Cerling, University of Utah, Salt Lake City, UT, and approved November 3, 2016 (received for review June 30, 2016)

December 27, 2016 114 (2) 251-256 https://doi.org/10.1073/pnas.1609112113

Significance

Lake Kivu is unusually stratified as a result of active volcanism nearby, with warmer, more saline water holding high concentrations of methane and CO_2, underlying cooler fresh water. We find that the history of carbonate sedimentation in Lake Kivu reflects the timing and duration of past hydrothermal input to the lake. The stable isotopic composition of aragonite ($CaCO_3$) and the lake's calcium budget reveal the strong link between hydrothermal input and aragonite deposition, which has occurred intermittently over just the past 3.1 ky. The sporadic injection of hydrothermal fluids and gases to the lake signals the difficulty of predicting future trends and potential for catastrophic degassing, which would be potentially fatal to >2 million people living near the lake shore.

Abstract

The sediment record of Lake Kivu reveals a complex volcanogenic and climatic Holocene history. Investigation of the inorganic carbonate record dates the onset of carbonate deposition in the mid-Holocene in Kivu's deep northern and eastern basins and identifies conditions enabling deposition. The magnitude and timing of carbonate-rich sedimentation is not so much controlled by climate but, instead, linked strongly to hydrothermal activity in the basin. Sublacustrine springs supply the vast majority of the calcium and carbonate ions required for supersaturation with respect to aragonite. This major hydrothermal activity that permanently stratifies Lake Kivu today was initiated ~3,100 y before present (3.1 ka), when carbonate-rich sediments first appeared in the Holocene record. Aragonite is the dominant $CaCO_3$ mineral present in the lake deposits. Both $\delta^{13}C$ and $\delta^{18}O$ of the aragonite are enriched above the expected kinetic fractionation of meteoric waters, suggesting a volcanogenic influence on the formation waters. Repeated major fluctuations in the carbonate record after 3.1 ka therefore most likely reflect the historical variation in hydrothermal inputs.

component of lake sediment is typically inorganic calcite or aragonite, which, by its presence, abundance, and isotopic composition, presents clues to past environmental conditions. The abundance of carbonate in lake sediment is determined by the ionic composition of the lake water, which often varies in response to the lake's hydrological budget, as well as by photosynthetic uptake of CO_2, which impacts the lake's pH (2). The carbon- and oxygen-stable isotopic composition of the carbonates can provide additional insight into the environment from which they precipitated in terms of past hydrological conditions (e.g., relatively arid or wet) and biological productivity (3), both of which may contribute to a regional paleoclimate record.

Located in the East African rift valley, Lake Kivu presents an unusual limnologic setting with active volcanism that impacts the lake water chemistry and density structure (4). Kivu consists of two deep basins (northern and eastern) with half-graben structure, and several smaller basins separated by a north−south trending plutonic sill (Fig. 1). Precambrian metamorphic bedrock underlies the lake basin, except along the northern shoreline, which abuts the active Virunga volcanic terrain. Degens et al. (4) suggest that Lake Kivu originally drained to the north into Lake Edward but subsequently was blocked by Late Pleistocene volcanic eruptions, resulting in the present drainage to the south via the Ruzizi River [into Lake Tanganyika with an average discharge of 3.6 $km^3 \cdot y^{-1}$ (5)]. The timing of this major reorganization of the lake's drainage is not known precisely because the putative volcanic damming to the north of the lake has not been dated. Strontium isotope data from a Lake Tanganyika core suggest that Kivu inflow to the lake began around 10.6 ka (6), and the highly serrated shoreline of Lake Kivu suggests that the catchment was flooded to this elevation in the relatively recent past. However, this could have resulted from volcanic damming to the north, or from a wetter climate in the Early Holocene as widely documented throughout East Africa (7, 8).

Fig. 1.

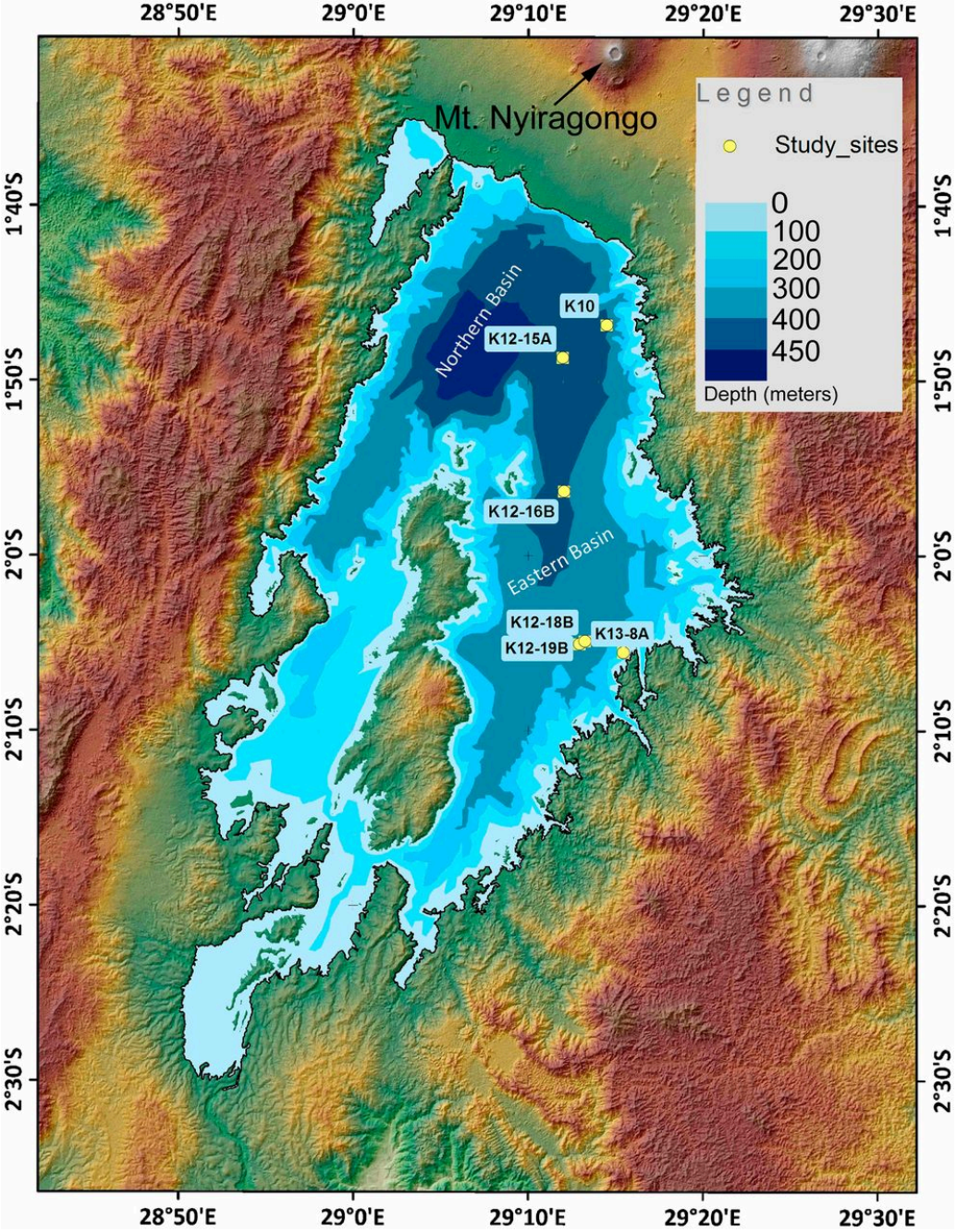

Topographic/bathymetric detail of Lake Kivu with coring sites (yellow circles) used in this study. Map created using ArcGis by Hubert Zal. Lake contours are in meters. Cores 19A and 19B were colocated and contemporaneous (only core 19B shown on the figure).

The carbonate deposition in Lake Kivu has varied in the recent past. There was an abrupt onset of aragonite accumulation in Kivu sediments just four decades ago, which continues to the present day. Pasche et al. (9) suggested this recent increase had three possible causes: (*i*) eutrophication of the upper water column, due to the introduction of a planktivorous sardine-like fish, *Limnothrissa miodon*, from Lake Tanganyika, which restructured the zooplankton community in a manner that enhanced lake primary production; (*ii*) greater nutrient input to the lake from anthropogenic activity in the catchment; or (*iii*) stronger upwelling of nutrient-rich deep waters as a result of a recent increase in sublacustrine hydrothermal spring discharge. However, Ross et al. (10) correctly pointed out that there were at least two earlier periods of abrupt onset and cessation of aragonite sedimentation in Lake Kivu over the past few thousand years (11) that could not be attributed to human influence but, instead, most likely reflected the influence of variable hydrothermal input to the lake. If this is true, then the Kivu record of carbonate sedimentation provides important insight into the history of hydrothermal influx to the deep northern basin. The deep waters of Lake Kivu contain dangerously high concentrations of CO_2 [300 km^3 at standard

to the north of the lake and of CH_4 (60 km^3 at STP) derived largely from H reduction of geogenic CO_2 in the deep water (12, 13). The methane concentrations would be supersaturated and spontaneously exsolve at lake surface conditions, but are stable at present in situ concentrations because of the strong density stratification of the lake imposed by saline, hydrothermal springs and the hydrostatic pressures in the monimolimnion as a consequence of the lake's depth. The density gradient of the water column is stable, yet unusual, with relatively warm saline waters derived from sublacustrine hydrothermal springs underlying fresher and cooler water above (4). The density structure could be destabilized by an abrupt increase in hydrothermal activity, perhaps associated with a magma eruption onto the lake floor, which would result in a catastrophic release of lethal gas to the ~2 million inhabitants living along the lake shore (13). Analysis of sediment cores allows historical reconstruction of past environmental events and may be the only way to establish whether catastrophic gas releases occurred in the past in Lake Kivu (11) and to assess the possibility of future limnologic eruptions.

Materials and Methods

Several gravity and Kullenberg piston cores were collected in January 2012 and March 2013 from the two deep basins of Lake Kivu (Fig. 1).

We analyzed three cores that were recovered in 2012–2013 from Lake Kivu (cores K12-19A and K12-19B both from 352 m depth, and core K13-8A from 96 m, hereafter referred to as cores 19A, 19B, and 8A, respectively; Fig. 1) for carbonate abundance, mineralogy, and isotopic composition (*Supporting Information*) to better understand the mechanisms that impact carbonate sedimentation in Lake Kivu and to refine the Holocene history of carbonate sedimentation in the lake. Prior research on carbonate deposition was based on analyses of short cores that span just the last few centuries (9, 10) or analyses of longer piston cores that were recovered in the early 1970s (14) but have questionable radiocarbon chronologies because of likely, but undefined, old carbon reservoir effects.

Results

Chronology.

Corrected radiocarbon dates on the six plant macrofossil samples in core 19A ranged from 3,635 ± 65 calendar years before present (cal y BP) at 348 cm below lake floor (blf) to 9,051 ± 40 cal y BP at 621 cm blf (Fig. S1). We also used a younger date of 2,172 ± 95 cal y BP in another piston core from Lake Kivu (K13-20A), which Zhang et al. (6) correlated stratigraphically to ~15 cm above the base of the lower carbonate interval in core 19A, i.e., at ~313 cm blf. We used these dates to construct an age model for this core (Fig. S1 and Table S1).

Fig. S1.

Radiocarbon dating of terrestrial macrofossils (diamonds); shown here as calibrated years before present (cal. ybp) versus depth in core 19A. Average LSR = 0.052 cm·y^{-1} before onset of carbonate deposition. Round symbols represent extrapolated rates from the regression to the bottom of core 19A ~12,700 cal y BP and to the onset of carbonate deposition at 3,150 cal y BP. The red square is based on stratigraphic correlation with a dated macrofossil in another core that is the youngest C-14 recovered from all Kivu cores (6). A higher sedimentation rate between onset of carbonate deposition and core surface is expected, as carbonate sediments have higher rates of sedimentation (refs. 12 and 22, Fig. 3) and upper sediments have higher water content.

Table S1.

Material analyzed for accelerator mass spectrometry ^{14}C ages for core K12-19A

Section	Depth (section), cm blf	Material	Radiocarbon age, ^{14}C y BP	Age, cal y BP
4	(55) 352.25	Twig	3,390 ± 30	3,635 ± 65
5	(12.5) 394.25	Twig	4,440 ± 30	5,104 ± 117
6	(45.5) 496.25	Twig	5,960 ± 30	6,800 ± 44
6	(94) 544.75	Twig	6,270 ± 40	7,212 ± 36
7	(18) 618.25	Macroplant	7,430 ± 40	8,265 ± 52
7	(35) 635.25	Macroplant	8,100 ± 40	9,051 ± 40
7	(89.5) 689.75	Macroplant	5,840 ± 30	6,650 ± 80 *

* Indicates samples excluded from regression in Fig. S1.

Carbonate Stratigraphy.

Core 19A reveals a dynamic Holocene history that began with the accumulation of coarse sands and

by organic-rich laminated, diatomaceous silty clays but with two prominent intervals of laminated calcareous silty clays, at 233 cm blf to 328 cm blf and at 154 cm blf to 198 cm blf. Several, generally thin, volcanic ash layers are scattered throughout the core (Fig. 2), as well as occasional turbidite deposits, often capped by diatomites (6). The sequence of major sediment lithologies in core 19A is consistent with, and stratigraphically correlated to, piston cores collected throughout the main eastern basin of the lake (Fig. S2). The two prominent carbonate layers in core 19A also align well with two carbonate horizons in core K10 recovered in 1971 from the North basin of the lake (ref. 11, Fig. 1). Gravity cores 19B (Fig. 3) and 8A (Fig. 4) reveal a similar alternating lithology between organic-rich, low carbonate, and carbonate-rich sediments separated by sharp, distinct contacts. Core 8A has relatively high carbonate, around 5% total inorganic carbon (TIC) (~40% $CaCO_3$), throughout the upper 55 cm of the core except for two short intervals at 20 cm blf to 22 cm blf and around 48 cm blf where TIC drops rapidly to total organic carbon (TOC)-rich sediment (Fig. 4). Core 19B also has two distinct TOC-rich short intervals, 35 cm blf to 38 cm blf and around 55 cm blf (Fig. 3), but, except for the uppermost 20 cm of the core, TIC is around 1% or less (<~12% $CaCO_3$). Overall, carbonate deposition has been higher and more continuous at the shallower coring site 8; this would be expected in a highly stratified lake in which the surface waters are supersaturated and the deep waters are not with respect to aragonite or calcite because of the hydrothermal influx of CO_2-rich, low-pH waters that are roughly >3 pH units lower than surface waters (13).

Fig. 2.

Core K12-19A image, stratigraphy, magnetic susceptibility (MS; SI, $\times 10^{-5}$), TOC (percent), TIC (percent), and stable isotopic composition of aragonite (permil relative to VPDB standard) versus depth from sediment top. Red ">" symbols are radiocarbon-dated macrofossils (cal y BP) with 1 SD. Lithology (Figs. 2–4): A, laminated, gray calcareous silty clay; B, laminated, brown-green diatomaceous silty clay; C, laminated, brown-orange sapropel; D, silty turbidite; E, Homogeneous, brown-green diatomaceous silty clay; F, massive, fine clay; and G, coarse sand and cobbles.

Fig. 3.

Core K12-19B image, stratigraphy, magnetic susceptibility (MS; SI, $\times 10^{-5}$), TOC (percent), TIC (percent), and stable isotopic composition (permil relative to VPDB standard) versus depth from sediment top.

Fig. 4.

crusts are illustrated with blue "∧" symbols in stratigraphy graphic. Apparent ash layer (red "∧") is evident as high magnetic susceptibility and low TOC and TIC.

Fig. S2.

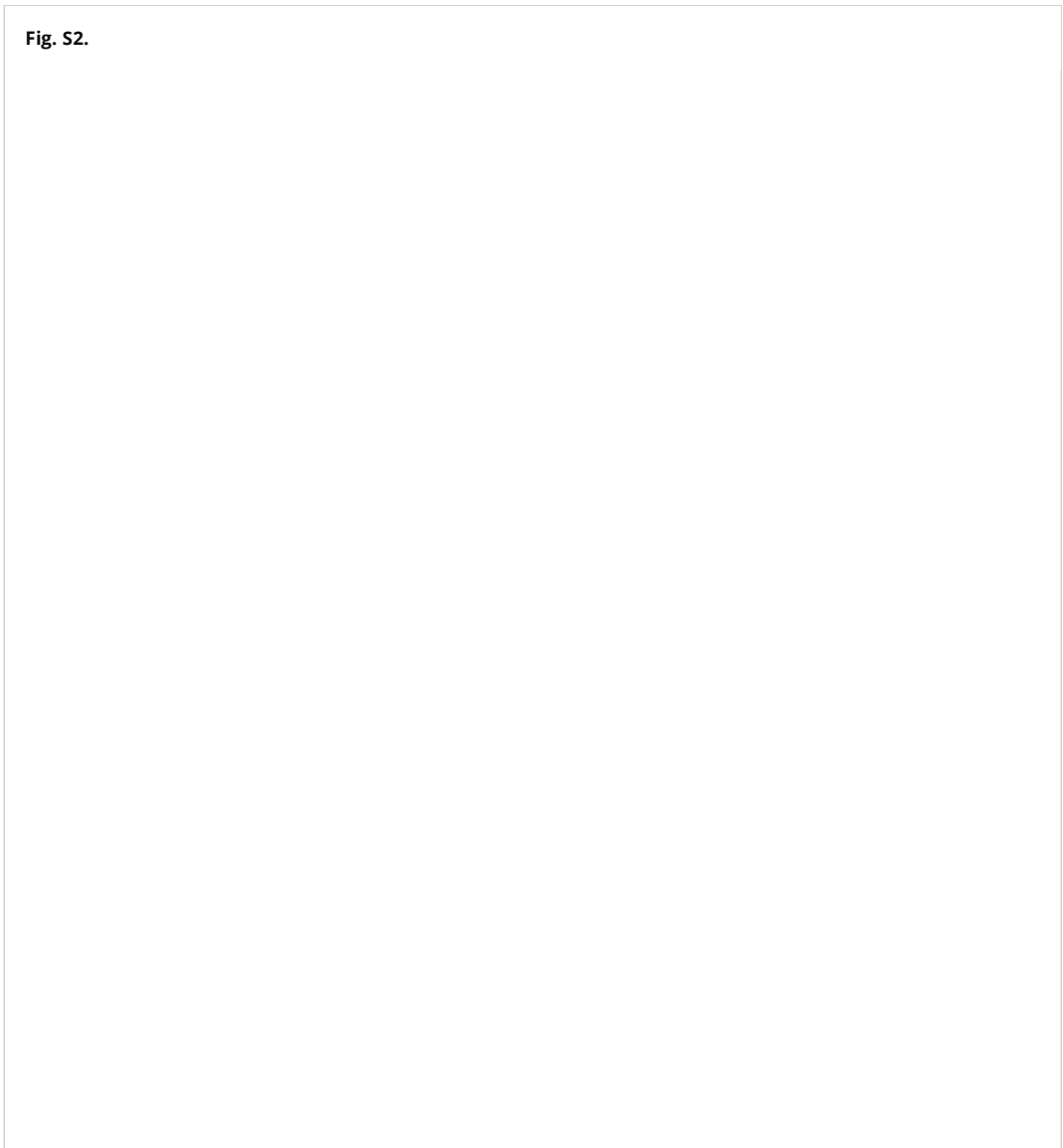

Stratigraphic correlation of cores K12-19A, K12-16B, and K12-15A reprinted with permission from ref. 6. with down-core depth scale in meters, which illustrates how the carbonate stratigraphy in core K12-19A is representative of the entire deep basin of Lake Kivu. Solid red (K12-19A) and black (other cores) circles illustrate radiocarbon samples and their respective dates. Gamma-ray attenuation density (g/cm^3) and magnetic susceptibility (MS; SI, ×10^{-5}) are shown next to core images and lithologic columns. Colored dashed lines correspond to swept-frequency seismic (Chirp) horizons (green denotes acoustic basement), and the black dashed lines correspond to volcanic ash layers. All cores are located in the eastern basin of Lake Kivu (Fig. 1).

The onset of carbonate deposition in core 19A at 328 cm blf, corresponding to ~3.1 ka by our age model (Fig. S1), indicates a major change from previous conditions in the Lake Kivu environment, as there was little or no carbonate deposited or preserved for thousands of years before 3.1 ka (Fig. 2). The few increases in TIC before 3.1 ka occur in turbidite intervals and do not represent the proximal pelagic environment. Carbonates continued to accumulate in the Lake Kivu deep sediments until about 2.2 ka (233 cm blf), when accumulation abruptly ceased, again indicating a major change in lake conditions. Calcareous deposition resumed from 198 cm blf to 154 cm blf, ~1.9–1.5 ka, when it again ceased abruptly. Carbonates appear again more recently in the companion gravity core 19B, although we do not have radiochronology from that core to determine when this occurred (Fig. 3). Core 8A contains two carbonate intervals, which very likely correspond to two carbonate horizons observed in each of the three short cores recovered from <200 m water depth in the North basin in 2006 (9) and 2010 (10) (Fig. 1). The lower carbonate interval between 53 cm and 13 cm depth terminated around AD 1900, and the other at the top

for the most recent carbonate deposition in core 8A to the interval of carbonate deposition before AD 1900 suggests that carbonate deposition had been nearly continuous at this shallower core site from AD 1580 to AD 1900, except for two brief intervals of noncalcareous sediment rich in organic carbon at 20 cm blf (estimated age AD 1850) and 47 cm blf (AD 1620) (Fig. S3). Ross et al. (10) also date the most recent onset of carbonate sedimentation to AD 1976, in excellent agreement with our dating on core 8A.

Fig. S3.

Lead-210 dating of bulk sediment from the upper 12 cm of core K13-8A. (Left) Excess ^{210}Pb activity. (Middle) Lithology: blue, calcareous sediment; dark brown, organic-rich, noncalcareous sediment. (Right) Year CE of deposition based on the CRS of the ^{210}Pb data (dots) and estimated sedimentation rate (horizontal bars) versus depth in core. Average CRS sediment flux = 173 g·m^{-2}·y^{-1}.

Carbonate Mineralogy and Isotopic Composition.

Our X-ray diffraction analyses revealed aragonite ($CaCO_3$) to be the dominant carbonate mineral present in all three cores, with lesser amounts of siderite ($FeCO_3$) occurring in some intervals. The presence of aragonite is consistent with the water chemistry of Lake Kivu; the upper 25 m of Lake Kivu presently have Mg and Ca concentrations of 84 mg/L and 7 mg/L (3.5 mM and 0.175 mM), respectively (15), with the molar ratio being well in excess of 12:1 required for $CaCO_3$ precipitation in the form of aragonite (16). Such high Mg:Ca ratios are unusual in dilute freshwater lakes; however, geochemical evolution in closed basin lakes can result in calcium carbonate deposition removing Ca while Mg becomes increasingly concentrated (17), accompanied by a shift from calcite to aragonite deposition.

The carbon and oxygen isotopic composition of aragonite covary down all three cores (Figs. 2–4) and plot at the more enriched end of the range of values that have been determined for lake carbonates (3) (Fig. 5). The $\delta^{18}O_{aragonite}$ values are similar to other African, albeit closed basin, lakes such as Turkana, Natron, and Bosumtwi. The $\delta^{13}C_{aragonite}$ values are more enriched in comparison with primary carbonates from other African lakes, thus indicating an isotopically enriched source of dissolved inorganic carbon (DIC) in Lake Kivu since the beginning of carbonate deposition and continuing to the present.

Fig. 5.

Cross-plot of $\delta^{13}C$ (y axis) and $\delta^{18}O$ (x axis) with all Lake Kivu carbonate data (this study) plotted in red-filled circles. For reference, primary carbonate data from other lakes around the world (3) are also plotted: closed lakes (filled symbols) and open lakes (open symbols).

Discussion

Onset of Carbonate Deposition in Lake Kivu.

Our study represents a nearly continuous sediment record of Lake Kivu spanning the past ~13,000 y, with a gross stratigraphy broadly similar to that described by Haberyan and Hecky (11) on cores recovered from Lake Kivu by the Woods Hole expeditions of 1971−1972. Stratigraphic overlap was not readily apparent between the base of either gravity core 19B or 8A and the uppermost portion of core 19A. Gas expansion disturbed and homogenized the uppermost 1.2 m of sediment in core 19A (Fig. 2), which prevents direct stratigraphic correlation between core 19A and the shorter cores. The gravity core 19B, taken as the trigger core of Kullenberg core 19A, did recover intact stratigraphy throughout its 65-cm length (Fig. 3). We can use the radiocarbon age model to estimate the age for the bottom of core 19B at ~0.6 ka. The mean linear sedimentation rate (LSR) over the Pb-210 dated interval in core 8A is 0.093 cm/y, and simple extrapolation would date the bottom of core 8A to be about 0.8 ka (Fig. S3). Core 19A is highly disturbed to 1.2 m, or to ~1.1 ka, and that indicates that we have a 300-y interval in which stratigraphic resolution has been obliterated by the gas expansion in core 19A. With that exception, the three cores together provide a high-resolution sedimentary record of environmental change in Lake Kivu back to 12.7 ka.

The coarse lithology at the base of our long core 19A indicates a lake low stand that may reflect the widespread aridity in East Africa during the Younger Dryas when most of the lakes of East Africa experienced low stands (7, 8). Haberyan and Hecky (11) reported coarse material, including cobble sized,

that water levels fell at least 380 m below the modern level 12,700 cal y BP, which would have placed the water level below our K19 coring site (Fig. 1). Laminated, organic-rich sediments overlying these sands suggest lake level rose quickly as the core site rapidly became more distal from near-shore sediment deposits. However, Lake Kivu remained a dilute lake for most of the Holocene, too dilute for precipitation of carbonate minerals in the deep water. Carbonate sedimentation began at 3.1 ka, with dramatic limnologic changes occurring, including the periodic cessation of calcareous sedimentation and the occasional deposition of distinctive, organic-rich brown layers. Our radiocarbon-based age model indicates that these changes in sedimentation were much more recent than reported by Haberyan and Hecky (11), who relied upon a few bulk radiocarbon dates from several cores to estimate an age of 9.4 ka for the onset of carbonate deposition. We suggest that their age model using bulk organic matter was affected by a substantial reservoir of dead carbon, as their only date near the top of the first interval of carbonate deposition was estimated as 6.2 ka. This date is much older than our radiocarbon-controlled date for a macrofossil recovered from just below the first carbonate interval of 3.635 ± 65 ka. Our radiocarbon model indicates that carbonate deposition began much more recently, at around 3.1 ka (328 cm blf), and ceased for the first time around 2.2 ka (233 cm blf). It has long been recognized that outflow from Lake Kivu has had a strong influence on the chemistry of Lake Tanganyika's water (18, 19). The onset of carbonate sedimentation in Lake Kivu slightly preceded the first appearance of carbonates in Lake Tanganyika sediment and a dramatic rise in the ^{14}C reservoir age of Lake Tanganyika water (20). The shift to more depleted $\delta^{18}O$ in Lake Tanganyika stromatolites around AD 500 (19) occurred when the second phase of carbonate sedimentation in Lake Kivu halted (1.5 ka).

Two main factors may have contributed to the timing of carbonate deposition in Lake Kivu: climate change and geothermal activity in the basin. The onset of carbonate deposition in the Kivu basin coincides roughly with the end of the African Humid Period (21), so it is conceivable that increased aridity in the region led to the lake becoming more saline and potentially supersaturated with respect to $CaCO_3$. On the other hand, we know that sublacustrine geothermal springs contribute significantly to the chemistry of Lake Kivu water (22) and likely are the cause of the isotopic enrichment of Lake Kivu aragonite that we observed. Is the history of carbonate accumulation in Lake Kivu the result of changing climate or hydrothermal input?

Factors Affecting Carbonate Sedimentation in Lake Kivu.

Here we consider the factors that caused the abrupt onset and subsequent appearance and disappearance during at least three intervals of carbonate deposition in the Kivu sediments.

The carbonate saturation index for natural waters is

$$\Omega = \log\left(\frac{[Ca^{2+}][CO_3^{2-}]}{K_c}\right), \quad [1]$$

where K_c is the temperature-dependent equilibrium constant for aragonite (or calcite), and $[Ca^{2+}]$ and CO_3^{2-} are ion activities (2). The system is supersaturated with respect to aragonite (or calcite) when $\Omega > 0$. Today, the surface waters in the main basin of Lake Kivu are supersaturated with respect to calcite (Ω = 0.72) and aragonite (Ω = 0.58), whereas the bottom waters are reported to be near equilibrium with respect to calcite (9, 10, 15). These Ω values are consistent with modern carbonate sediments being found in gravity cores from this study and others (9, 10) at lake depths of up to 350 m at site 19, as well as deposits along the modern shoreline in the form of beach rock.

Calcareous sediments did not accumulate in the deep basins of Kivu for most of its Holocene history. The bedrock geology of Lake Kivu is nearly devoid of limestone or other Ca-rich lithology (15), so Ca concentration in surface runoff would be dilute in this high-rainfall region, >1,400 mm/y (5). The volcanic

rainfall quickly enters the groundwater (23). The Kagera River, which arises immediately to the east of the drainage divide of the Lake Kivu basin, may be considered representative of Kivu basin surface waters draining metamorphic basement lithology and has reported Ca concentration of 0.13 mmol·L^{-1} and similarly low alkalinity, 0.79 mmol·L^{-1} (24) which, together, would give a saturation index well below 0. Evaporation can raise Ca concentrations relative to inflowing concentrations, and can be especially strong in closed basin lakes (17). Lake Kivu is not a closed basin lake and has a major outflow via the Ruzizi River, so evaporation only accounts for 54% of water loss (5). Such a water balance would imply that inflowing surface waters would only be concentrated by a factor of 2 in the modern lake. The lake has likely had its outflow since the Early Holocene. Strong variations in evaporative concentration are unlikely to have driven a Late Holocene increase in carbonate deposition at 3.1 ka, nor is there evidence of substantial changes to the water budget in the Late Holocene that would account for the repeated onset and cessation observed. Some other mechanism of enriching Ca^{+2} and CO_3^{2-} must drive up the saturation index in Lake Kivu causing aragonite precipitation and the high alkalinity in the lake's surface water today, which exceeds 12 mmol·L^{-1}, well in excess of what evaporative concentration of surface runoff could accomplish.

The answer lies in analysis of the calcium budget of the lake (Table S2). From this budget, we find that the Ruzizi River annually exports nearly 50% more calcium (1.66×10^7 kg Ca·y^{-1}) from Lake Kivu than it receives from surface inflows (1.2×10^7 kg Ca·y^{-1}), and hydrothermal springs contribute an order of magnitude more Ca to the annual budget (11.0×10^7 kg Ca·y^{-1}) than do surface streams.

Table S2.

Lake Kivu calcium budget

Flux	Source	[Ca^{2+}],* mg/L	Flow rate,† km^3/y	Annual amount, kg Ca/y	Potential sed flux,‡ g Ca·m^{-2}·y^{-1}
In	Surface streams	5	2.4	1.2×10^7	
	Hydrothermal springs	89	1.3	11.0×10^7	
Out	Ruzizi River	4.6	3.6	1.7×10^7	
Sedimented				10.5×10^7	44.35

* Concentration from Ross et al. (10) with hydrothermal springs [Ca^{2+}] as mean of five unique spring inflows and from Kilham and Hecky (24) for characteristic value for surface runoff.

† Surface stream discharge compiled from 21 rivers by Muvundja et al. (5), hydrothermal seeps from *Schmid* et al. (13), and outlet measured at Ruzizi I Hydropower Plant (1941–2005).

‡ Potential sediment flux (sed flux) assumes uniform Ca burial rate across the entire lake floor area (2.37×10^9 m^2).

A sedimentation flux (grams of Ca per square meter per year) was calculated from the estimate of total Ca^{2+} accumulated in the basin (i.e., the inputs minus the outputs, 10.5×10^7 kg Ca·y^{-1}), assuming that $CaCO_3$ was deposited uniformly across the entire lake floor area (using lake surface area: 2.37×10^9 m^2). This yields a value of 44.35 g Ca·m^{-2}·y^{-1}, which can be compared with actual calcium mass accumulation rates (MARs) calculated from our sediment cores (Table S3). The higher Ca flux rates in the shallower core 8A (~41 g Ca·m^{-2}·y^{-1} to 46 g Ca·m^{-2}·y^{-1}) agree well with our Ca budget estimate of flux (~44 g Ca·m^{-2}·y^{-1}), whereas the deep-water sedimentation flux is lower (~12 g Ca·m^{-2}·y^{-1} to 14 g Ca·m^{-2}·y^{-1}) (*Supporting Information*). This finding would be expected, as the sedimentary flux offshore settles into deeper water and is exposed to lower pH than surface waters, and therefore some dissolution will occur before burial.

than in core 19B (Fig. 3). Dissolution during sedimentation of carbonate produced in surface waters accounts for higher dissolved Ca concentrations in the deeper water column than were measured at inflowing springs (10). Consequently, we suggest that the Ca sedimentary flux to core 8A is more representative of surface water fluxes than that to core 19B. Ca sedimentary flux would be even higher at shallower depths and higher pH [>9 (9)] and along shorelines where $CaCO_3$ precipitates onto solid surfaces today. Although the MAR_{Ca} values calculated for cores 19A and 8A cannot be assumed to be representative of the whole lake, our calculations at least demonstrate the right order of magnitude of Ca burial rate in the lake to achieve a balance of the estimated Ca budget, in which hydrothermal input and sediment burial are by far the dominant terms. Hydrothermal springs are essential for deposition of $CaCO_3$ in Lake Kivu sediments.

Table S3.

Carbonate mass accumulation rates and Ca^{2+} flux

Core - lithology	Depth interval, cm	ρ, g/cm^3	LSR, cm/y	MAR, g·m^{-2}·y^{-1}	TIC, %	Ca, %	MAR_{Ca}, g Ca·m^{-2}·y^{-1}	Annual, kg Ca/y
8A - carbonate	0–5	2.37	0.12	227.5	5.43	18.1	41.18	9.8×10^7
8A - carbonate	25–40.5	2.31	0.12	194.0	7.15	23.8	46.25	11.0×10^7
19A - carbonate	158–198	2.09	0.1	104.5	4.07	13.6	14.17	3.4×10^7
19A - carbonate	235–327.5	1.97	0.058	115.7	3.23	10.8	12.46	2.95×10^7

Estimates are from the carbonate intervals of K13-8A and K12-19A. Estimates of ρ and φ are from Votava (36). Porosity values used are as follows: 0.92 (8A, 0 cm to 5 cm); 0.93 (8A, 25 cm to 40.5 cm); 0.95 (19A, 158 cm to 198 cm); and 0.89 (19A, 235 cm to 327.5 cm).

If the sublacustrine springs were to stop contributing calcium to the water column, the response time of the lake would be about 300 y (*Supporting Information*). Thus, it should take a few centuries for current rates of Ca deposition to drive the lake to undersaturation with respect to aragonite if hydrothermal inputs stopped. An interval of 300 y would represent ~30 cm of sedimentation at the LSR in cores 8A and 19B. The rapid termination of aragonite sedimentation evident in the sharp contacts between carbonate and noncarbonate strata in three intervals in our cores over the last 3,000 y suggests that a critical threshold for preservation is surpassed rather than a steady decline in carbonate precipitation and most likely accounts for the rapid termination of carbonate deposition. The carbonate record at core 8A indicates that carbonate deposition ceased within a few years around 1900 AD and then resumed after a 75-y hiatus. The most recent (since 1975) rapid onset of carbonate sedimentation in both the shallower core 8A and the deeper core 19B would appear to require an increase in pH extending from the deep water at 352 m and up to 90 m depth and/or an increased rate of Ca input from the deep water where sublacustrine springs occur. The unique thermohaline density stratification of the main basin has persisted for the past 75 y (25), so significantly increased vertical transport of Ca and CO_2 is unlikely. However, the discharge rate, and especially the CO_2 concentrations in the sublacustrine springs that maintain the vertical thermohaline structure, may vary over time in response to the degassing of the deep magma chamber feeding the Virunga Volcanoes and the possibly changing pathways that the CO_2 gas emissions follow to interact with the groundwater system.

The Isotopic Composition of Lake Kivu Aragonite.

We compare the measured values to the expected values of $\delta^{18}O_{aragonite}$ by kinetic fractionation based on the following relationship (26):

$$1{,}000 \quad \ln\alpha_{a-w} = 17.88 \pm 0.13(1{,}000)/T - 31.14 \pm 0.46, \qquad [2]$$

where

$$\alpha_{a-w} = \frac{(1{,}000 + \delta^{18}O_{aragonite})}{(1{,}000 + \delta^{18}O_{water})}, \qquad [3]$$

and temperature (T) is in kelvin, α is the fractionation factor, and $\delta^{18}O$ is in permil deviation from Vienna Standard Mean Ocean Water (VSMOW).

Applying modern-day $\delta^{18}O_{water}$ values reported by Ross et al. (10) of about 3.9‰ VSMOW for surface water in the main basin of the lake yields an equilibrium $\delta^{18}O_{aragonite}$ value of 2.7‰ Vienna PeeDee Belemnite (VPDB), which nearly equals the measured values of ~2.5‰ VPDB from the tops of cores 8A and 19B.

Both the oxygen and carbon isotopes of Lake Kivu aragonite display more enriched values than the primary carbonates from other lakes (Fig. 5). Equilibrium values of $\delta^{13}C_{aragonite}$ were calculated from $\delta^{13}C_{CO2(volcanogenic)}$ following the relationship (27)

$$\delta^{13}C_{CaCO_3} = (\delta^{13}C_{CO_2} + 1{,}000) \times 1.01017 - 1{,}000, \qquad [4]$$

with temperature at 25 °C.

Tedesco et al. (28) report $\delta^{13}C_{CO2}$ from fumarolic gas samples collected within Nyiragongo crater (about 20 km north of Lake Kivu) of −3.65‰. Applying this value to Eq. **4** yields a $\delta^{13}C_{aragonite}$ of 6.48‰, which is similar to the measured values from the top 1 cm of cores 8A and 19B: 6.23‰ and 6.29‰, respectively. Atmospheric or biogenic sources of $\delta^{13}C_{CO2}$ are generally depleted to −7‰ or less (29).

Equilibrium values of $\delta^{13}C_{aragonite}$ were also calculated from the following relationship (27):

$$\delta^{13}C_{CaCO_3} = (\delta^{13}C_{DIC} + 1{,}000) \times 1.00185 - 1{,}000, \qquad [5]$$

where $\delta^{13}C_{DIC}$ is the isotopic composition of the DIC of the formation waters at 25 °C.

Tassi et al. (15) report a single measured value of 3.35‰ $\delta^{13}C_{DIC}$ for the surface waters of the main basin, which would yield a $\delta^{13}C_{aragonite}$ value of 5.21‰, which is lower than the measured values in cores 8A and 19B. The core 8A carbonate stratigraphy is quite enriched in $\delta^{13}C_{aragonite}$, especially in the vicinity of aragonitic crusts (Fig. 4, 27 cm blf to 20 cm blf, corresponding to ~AD 1740–1800, extrapolated from the ^{210}Pb age model), with $\delta^{13}C_{aragonite}$ reaching 8.62‰, suggesting more enriched DIC in the surface waters than today. The enriched values of Kivu's $\delta^{13}C_{aragonite}$ compared with other African lake carbonates largely demonstrate the influence of local volcanogenic CO_2 on carbonate sedimentation in Lake Kivu.

The isotopically enriched aragonite that has accumulated on and off in Lake Kivu since 3.1 ka indicates that geogenic CO_2 has dominated the $\delta^{13}C$ composition of DIC and CO_2 in the Lake Kivu water column throughout the periods of carbonate deposition. The intervening intervals of noncarbonate deposition indicate that the fluxes of groundwater and/or CO_2 flux have not been constant over time. Ca delivery by the hydrothermal springs is dependent on chemical weathering of the volcanic rock and the groundwater flux, whereas the fluxes of CO_2 and heat can vary independently of the groundwater discharge and weathering. The geologic structures and processes around and under Kivu are dynamic. Variability in

and volcanic activity increasing CO_2 and heat flux, or both, which, in turn, would alter the precipitation and preservation of aragonite.

We observe no clear relationship between ash layers in our cores (i.e., stratigraphic evidence of volcanic activity) and the relative timing of carbonate deposition. Our long core 19A contains ash layers throughout the Holocence, with more recent layers occurring before, or at the initiation of, carbonate deposition (Fig. 2). Our short cores, however, show no clear relationship (Figs. 3 and 4). These observations are not consistent with those of Ross et al. (10), who reported ash layers associated with the termination of carbonate deposition in their cores.

Conclusion

The presence of carbonate layers in the sediments of many of the East African Great Lakes indicates relatively arid climate conditions at the time of their accumulation (e.g., refs. 20 and 30–32). However, our study indicates that the aragonitic sediments of Lake Kivu reflect a history of hydrothermal activity in the lake basin, rather than climate change, and are broadly consistent with the conclusions of Ross et al. (10). However, we demonstrate that the hydrothermal impact on Lake Kivu is a much more recent phenomenon than previously reported (11), with onset occurring at about 3.1 ka. Since the original episode of carbonate deposition, there have been at least three hiatuses and subsequent resumptions, most recently in about AD 1975. Isotopic analyses of the endogenic aragonite indicate that a geogenic source of CO_2 dominates the DIC composition in the lake. Our calculations of $CaCO_3$ MARs and estimated sources and sinks of Ca within the lake system demonstrate a Ca budget for the lake that is currently heavily dominated by hydrothermal input and deposition of aragonite. Once initiated, and given current rates of inflow, hydrothermal springs supply the lake with a large reservoir of Ca and CO_2, with a Ca residence time of about 300 y. The stratigraphic record indicates rapid onset and termination of calcareous intervals, which suggests a mechanism linked to volcanogenic, rather than climatic, events. There is substantial complexity in the Kivu system, and further understanding of the mechanisms and variability of hydrothermal spring input is essential to evaluating the risk of catastrophic degassing at some future time.

SI Text

Core Sampling and Analyses.

All cores were sent to the LacCore facility at University of Minnesota in Minneapolis, where they were logged on a GeoTek MSCL-XYZ multisensor core logger, split longitudinally, examined for macrofossils, and visually described for changes in composition. An 856-cm-long core (core 19A, 352 m water depth) from the eastern basin was chosen to study in detail after seismic and sedimentological analyses confirmed the presence of thick (>10 cm) turbidite sequences, which complicated stratigraphic analysis in many of the other cores that had been recovered from greater depths in the northern basin (6). Additionally, the accompanying trigger gravity core 19B (68 cm long) and another gravity core, 8A (73 cm long; recovered from 96 m water depth) were selected for this study to provide greater resolution of the recent record. The latter core from relatively shallow water was analyzed, because most deep-water cores from Lake Kivu are greatly disturbed in their upper centimeters by degassing of methane and CO_2 upon retrieval from great depth.

Approximately 1 cm^3 to 2 cm^3 of wet material were sampled at 1- to 5-cm intervals in the cores, freeze-dried, and then homogenized by agate mortar and pestle. Total carbon and TIC were determined on a UIC Coulometer Carbon Furnace CM5300 (950 °C) and Acidification Module CM5130, respectively. TOC was determined by loss on ignition using a modified version of ref. 33. The carbonate mineralogy was

identified with the software suite X'Pert High Score. Aragonite-rich sediments in the <63-μm fraction were analyzed for carbon and oxygen isotopes by first removing organic matter in a 2.625% NaOCl solution overnight, rinsed, and then air-dried (modified from ref. 34). Treated samples were sent to Dr. David Dettman at the University of Arizona's Environmental Isotope Laboratory for isotopic analysis. The results are reported as $\delta^{13}C_{aragonite}$ and $\delta^{18}O_{aragonite}$ in permil deviation from VPDB, with a precision of <0.1‰.

Geochronology.

We recovered terrestrial macrofossils at six depths in core 19A, which were radiocarbon dated by accelerator mass spectrometry at Beta Analytics. Radiocarbon dates were converted to years before present using CalPal^{online} (www.calpal-online.de) (Table S1). The age model for core 19A was established by applying a linear regression through the radiocarbon dates from the base of the core to 328 cm blf (i.e., onset of the first major carbonate interval), and linear extrapolation from the assigned date at 328 cm blf to 0 age at the core top (Fig. S1). The sedimentation rate before onset of carbonate deposition was remarkably invariant, with an LSR of 0.053 cm·y^{-1}, and interpolating from the onset of carbonate deposition to the lake bottom renders an LSR of 0.106 cm·y^{-1}. The higher LSR in the carbonate-containing strata is consistent with results of Pasche et al. (9), Ross et al. (10), and our own Pb-210 results for carbonate-rich and carbonate-poor strata in core 8A (Fig. S3).

Lead-210 geochronology was used for the recent (<120 y) sediments of core 8A, through the determination of excess ^{210}Pb by alpha spectroscopy at the University of Manitoba Department of Soil Science. Excess ^{210}Pb activity in core 8A ranged from 1.45 Bq·g^{-1} at the core top to 0.02 Bq·g^{-1} at 11.5 cm depth. A sediment depth–age relation was established using the constant rate of supply (CRS) model (35), given the minimal bioturbation at the coring site due to overlying anoxic water (Fig. S3). The ^{210}Pb-dated interval indicated a mean LSR for the interval of 0 cm to 12 cm of 0.093 cm·y^{-1}, with higher rates in calcareous intervals, LSR = 0.124 cm·y^{-1}, but lower in noncalcareous sediments, LSR = 0.091 cm·y^{-1}. If the mean LSR for the dated interval is applied to the length of core 8A, the bottom of the core would have an estimated age of 800 y BP.

Calcium Budget for Lake Kivu.

We construct a simple budget based on reported discharge and solute concentrations from surface tributaries, subaquatic hydrothermal springs, and the Ruzizi River (Table S2) (5, 10, 13, 24). We tally the annual contributions and losses of Ca to/from the lake by rivers and hydrothermal sources to estimate the amount of calcium that must accumulate in the lake sediments, assuming steady state (Table S3).

Calcium MARs Measured in Lake Kivu.

Calcium MARs (grams Ca per square meter per year, MAR_{Ca}) were calculated from cores 19A and 8A for various intervals using sediment dry bulk density ($\rho_{dry\ bulk}$), porosity (φ), and LSR,

$$MAR_{Ca} = MAR\frac{\%\ Ca}{100}, \quad [S1]$$

where

$$MAR = LSR\times(1-\phi)\times\rho_{dry\ bulk}, \quad [S2]$$

and, assuming all TIC measured is $CaCO_3$,

$$\%\ Ca = \frac{\%\ TIC}{0.12}\times 0.4, \quad [S3]$$

and 0.12 and 0.4 reflect the stoichiometric proportions of C and Ca, respectively.

LSR estimates came from the appropriate age model: 0.053 $cm \cdot y^{-1}$ for core 19A for a depth of >328 cm blf, 0.1 $cm \cdot y^{-1}$ for depths of <328 cm blf, and 0.12 $cm \cdot y^{-1}$ for core 8A (Figs. S1 and S3).

Calculating the Ca Residence Time in Lake Kivu.

$$\text{Ca residence time} = \left(\frac{[Ca^{2+}] \times \text{lake volume}}{\text{Ca input rate}}\right), \quad [S4]$$

where $[Ca^{2+}]$ equals 57.5×10^6 kg $Ca \cdot km^{-3}$ [water column mean calculated from main basin values reported by Tassi et al. (15)], lake volume equals 560 km^3 (5), and the Ca input equals 12.2×10^7 kg $Ca \cdot y^{-1}$ (Table S3). The residence time of Ca in Lake Kivu is found to be on the order of 300 y.

Acknowledgments

Research funding was provided by MacArthur Foundation Grant 11-97251-000-INP "Dynamics of the Lake Kivu System: Geological, Biological and Hydrographic Impacts on Biodiversity and Human Wellbeing" and by a Regents Professor Research Fund of the University of Minnesota (to T.C.J.).

Supporting Information

Supporting Information (PDF)

Supporting Information

DOWNLOAD | 541.44 KB

References

1 TC Johnson, Sedimentary processes and signals of past climatic change in the large lakes of the East African Rift Valley. *The Limnology, Climatology and Paleoclimatology of the East African Lakes*, eds TC Johnson, EO Odada (Gordon and Breach, Amsterdam), pp. 367–412 (1996).
Google Scholar

2 K Kelts, KJ Hsu, Freshwater carbonate sedimentation. *Lakes: Chemistry, Geology, Physics*, ed A Lerman (Springer, New York), pp. 295–324 (1978).
Crossref | Google Scholar

3 MR Talbot, A review of the paleohydrological interpretation of carbon and oxygen isotopic ratios in primary lacustrine carbonates. *Chem Geol* **80**, 261–279 (1990).
Google Scholar

4 ET Degens, RPV Herzen, H-K Wong, WG Deuser, HW Jannasch, Lake Kivu: Structure, chemistry and biology of an east African rift lake. *Geol Rundsch* **62**, 245–277 (1973).
Crossref | Google Scholar

5 FA Muvundja, et al., Balancing nutrient inputs to Lake Kivu. *J Great Lakes Res* **35**, 406–418 (2009).
Crossref | Google Scholar

6 X Zhang, et al., Climatic control of the late Quaternary turbidite sedimentology of Lake Kivu, East Africa: Implications for deep mixing and geologic hazards. *Geology* **42**, 811–814 (2014).
Crossref | Google Scholar

Crossref | Google Scholar

8 MA Berke, et al., Characterization of the last deglacial transition in tropical East Africa: Insights from Lake Albert. *Palaeogeogr Palaeoclimatol Palaeoecol* **409**, 1–8 (2014).

Crossref | Google Scholar

9 N Pasche, et al., Abrupt onset of carbonate deposition in Lake Kivu during the 1960s: Response to recent environmental changes. *J Paleolimnol* **44**, 931–946 (2010).

Crossref | Google Scholar

10 KA Ross, M Schmid, S Ogorka, FA Muvundja, FS Anselmetti, The history of subaquatic volcanism recorded in the sediments of Lake Kivu; East Africa. *J Paleolimnol* **54**, 137–152 (2015).

Crossref | Google Scholar

11 KA Haberyan, RE Hecky, The late Pleistocene and Holocene stratigraphy and paleolimnology of Lakes Kivu and Tanganyika. *Palaeogeogr Palaeoclimatol Palaeoecol* **61**, 169–197 (1987).

Crossref | Google Scholar

12 N Pasche, et al., Methane sources and sinks in Lake Kivu. *J Geophys Res* **116**, G03006 (2011).

Crossref | Google Scholar

13 M Schmid, M Halbwachs, B Wehrli, A Wuest, Weak mixing in Lake Kivu: New insights indicate increasing risk of uncontrolled gas eruption. *Geochem Geophys Geosyst* **6**, Q07009 (2005).

Crossref | Google Scholar

14 P Stoffers, RE Hecky, Late Pleistocene−Holocene evolution of the Kivu−Tanganyika basin. *Modern and Ancient Lake Sediments*, International Association of Sedimentologists Special Publication, eds Matter A, Tucker ME (Blackwell Sci, Oxford), Vol 2, pp 43–55. (1978).

Google Scholar

15 F Tassi, et al., Water and gas chemistry at Lake Kivu (DRC): Geochemical evidence of vertical and horizontal heterogeneities in a multibasin structure. *Geochem Geophys Geosyst* **10**, Q02005 (2009).

Crossref | Google Scholar

16 G Müller, G Irion, U Forstner, Formation and diagenesis of inorganic Ca−Mg carbonates in the lacustrine environment. *Naturwissenschaften* **59**, 158–164 (1972).

Crossref | Google Scholar

17 P Kilham, Mechanisms controlling the chemical composition of lakes and rivers: Data from Africa. *Limnol Oceanogr* **35**, 80–83 (1990).

Crossref | Google Scholar

18 P Stoffers, RE Hecky, Late-Pleistocene and Holocene evolution of the Kivu-Tanganyika basin. *Modern and Ancient Lake Sediments*, International Association of Sedimentologists Special Publication, eds Matter A, Tucker ME (Blackwell Sci, Oxford), Vol 2, pp 43–55. (1978).

Google Scholar

19 AS Cohen, M Talbot, SM Awramik, DL Dettman, P Abell, Lake level and paleoenvironmental history of Lake Tanganyika, Africa, as inferred from late Holocene and modern stromatolites. *Geol Soc Am Bull*

20 A Felton, et al., Paleolimnological evidence for the onset and termination of glacial aridity from Lake Tanganyika, tropical East Africa. *Palaeogeogr Palaeoclimatol Palaeoecol* **252**, 405–423 (2007).

Crossref | Google Scholar

21 P deMenocal, et al., Abrupt onset and termination of the African Humid Period: Rapid climate responses to gradual insolation forcing. *Quat Sci Rev* **19**, 347–361 (2000).

Crossref | Google Scholar

22 KA Ross, et al., Lake-level rise in the late Pleistocene and active subaquatic volcanism since the Holocene in Lake Kivu, East African Rift. *Geomorphology* **221**, 274–285 (2014).

Crossref | Google Scholar

23 CM Balagazi, et al., River geochemistry, chemical weathering, and atmospheric CO_2 consumption rates in the Virunga Volcanic Province (East Africa). *Geochem Geophys Geosyst* **16**, 2637–2660 (2015).

Crossref | Google Scholar

24 P Kilham, RE Hecky, Fluoride: Geochemical and ecological significance in East African waters and sediments. *Limnol Oceanogr* **18**, 932–945 (1973).

Crossref | Google Scholar

25 S Katsev, AA Aaberg, SA Crowe, RE Hecky, Recent warming of lake Kivu. *PLoS One* **9**, e109084 (2014).

Crossref | PubMed | Google Scholar

26 S-T Kim, JR O'Neil, C Hillaire-Marcel, A Mucci, Oxygen isotope fractionation between synthetic aragonite and water: Influence of temperature and Mg2+ concentration. *Geochim Cosmochim Acta* **71**, 4704–4715 (2007).

Crossref | Google Scholar

27 G Faure *Principles of Isotope Geology* (John Wiley, Hoboken, NJ, 1986).

Google Scholar

28 D Tedesco, et al., Gas isotopic signatures (He, C, and Ar) in the Lake Kivu region (western branch of the East African rift system): Geodynamic and volcanological implications. *J Geophys Res Solid Earth* **115**, B01205 (2010).

Crossref | Google Scholar

29 MJ Leng, AT Marshall, Palaeoclimate interpretation of stable isotope data from lake sediment archives. *Quat Sci Rev* **23**, 811–831 (2004).

Crossref | Google Scholar

30 JD Halfman, High-resolution sedimentology and paleoclimatology of Lake Turkana, Kenya. PhD dissertation (Duke Univ, Durham, NC). (1987).

Google Scholar

31 BP Finney, CA Scholz, TC Johnson, S Trumbore, J Southon, Late Quaternary lake-level changes of Lake Malawi. *The Limnology, Climatology, and Palaeoclimatology of the East African Lakes*, eds TC Johnson, EO Odada (Gordon and Breach, Toronto), pp. 495–508 (1996).

Google Scholar

32 JD Halfman, TC Johnson, BP Finney, New AMS dates, stratigraphic correlations and decadal climatic cycles for the past 4 ka at Lake Turkana, Kenya. *Palaeogeogr Palaeoclimatol Palaeoecol* **111**, 83–98 (1994).

Crossref | Google Scholar

33 O Heiri, AF Lotter, G Lemcke, Loss on ignition as a method for estimating organic and carbonate content in sediments: Reproducibility and comparability of results. *J Paleolimnol* **25**, 101–110 (2001).

Crossref | Google Scholar

34 BA Steinman, MB Abbott, Isotopic and hydrologic responses of small, closed lakes to climate variability: Hydroclimate reconstructions from lake sediment oxygen isotope records and mass balance models. *Geochim Cosmochim Acta* **105**, 342–359 (2013).

Crossref | Google Scholar

35 PG Appleby, Chronostratigraphic techniques in recent sediments. Tracking Environmental Change Using Lake Sediments Vol. 1: Basin Analysis, Coring, and Chronological Techniques, eds Last WM, Smol JP (Kluwer, Dordrecht, The Netherlands), pp 171−203. (2001).

Google Scholar

36 JE Votava, The Holocene history of Lake Kivu (East Africa): New perspectives from new cores. MS thesis (Univ Minnesota Duluth, Duluth, MN). (2014).

Google Scholar

Gayatri Mishra

Resolving Feynman's restaurant problem reveals optimal solutions and human strategies

Richard Feynman described a decision-making problem and its solution in handwritten notes, but the meaning of the…

RESEARCH ARTICLE | MAY 19, 2026 |

Ethan Eldridge, Evan M. Russek, and Thomas L. Griffiths

Large language models pass a standard three-party Turing test

The Turing test asks whether a machine can imitate human behavior so well that another human cannot reliably tell the…

Cameron R. Jones and Benjamin K. Bergen